

Research Article

Novel Mixed EWMA Dual-Crosier CUSUM Mean Charts without and with Auxiliary Information

Muhammad Arslan ¹, Muhammad Azeem Ashraf ¹, Syed Masroor Anwar ²,
Zahid Rasheed ³, Xuelong Hu ⁴, and Saddam Akbar Abbasi ^{5,6}

¹Research Institute of Educational Science, Hunan University, Changsha, China

²Department of Statistics, University of Azad Jammu and Kashmir, Muzaffarabad, Pakistan

³Department of Mathematics, Women University of Azad Jammu and Kashmir, Bagh, Pakistan

⁴School of Management, Nanjing University of Posts and Telecommunications, Nanjing, China

⁵Statistics Program, Department of Mathematics, Statistics, and Physics, College of Arts and Science, Qatar University, Doha 2713, Qatar

⁶Statistical Consulting Unit, College of Arts and Science, Qatar University, Doha 2713, Qatar

Correspondence should be addressed to Muhammad Azeem Ashraf; azeem20037@gmail.com

Received 29 August 2021; Revised 29 October 2021; Accepted 29 January 2022; Published 29 March 2022

Academic Editor: Thomas Hanne

Copyright © 2022 Muhammad Arslan et al. This is an open access article distributed under the Creative Commons Attribution License, which permits unrestricted use, distribution, and reproduction in any medium, provided the original work is properly cited.

The classical cumulative SUM (CUSUM) chart is commonly used to monitor a particular size of the mean shift. In many real processes, it is assumed that the shift level varies within a range, and the exact level of the shift size is mostly unknown. For detecting a range of shift size, the dual-CUSUM (DC) and dual-Crosier CUSUM (DCC) charts are used to provide better detection ability as compared to the CUSUM and Crosier CUSUM (CC) charts, respectively. This paper introduces a new mixed exponentially weighted moving average (EWMA)-DCC (EDCC) chart to monitor process mean. In addition, AIB-based EWMA-DC (EDC) and EDCC charts (namely, AIB-EDC and AIB-EDCC charts) are suggested to detect shifts in the process mean level. Monte Carlo simulations are used to compute the run length (RL) characteristics of the proposed charts. A detailed comparison of the proposed schemes with other competing charts is also provided. It turns out that the proposed chart provides better performance than the counterparts when detecting a range of mean shift sizes. A real-life application is also presented to illustrate the implementation of the existing and proposed charts.

1. Introduction

Statistical process monitoring (SPM) provides many techniques to help practitioners monitor the manufacturing or industrial processes for assignable causes of variation. Control charts are a widely used SPM technique to detect the process shifts by assignable causes and also to help to establish the process capability. Shewhart and Van Nostrand [1] introduced a memoryless control chart used to monitor large shifts in a process parameter. Regardless of the wide prominence and simplicity of the Shewhart charts, these charts are ineffective in industries or manufacturing processes where small shifts occur. Therefore, the memory-type

control charts, including the cumulative sum (CUSUM) by Page [2] and the exponentially weighted moving average (EWMA) control chart by Roberts [3], are widely used to deal with the sooner detection of small to moderate shifts.

In SPM, it is a common practice to enhance the sensitivity of the control chart with the induction of an auxiliary information-based (AIB) estimator of the underlying process parameter(s). Abbas et al. [4] enhanced the detection ability of the classical EWMA chart and suggested the AIB-EWMA chart. The AIB-EWMA mean chart significantly and uniformly outperforms the classical EWMA mean chart. Likewise, Haq [5] and Abbasi and Haq [6] suggested adaptive EWMA and adaptive CUSUM charts for the

process mean when the shift is not known in advance. Similarly, Haq and Khoo [7] suggested a multivariate process mean chart using auxiliary information. In order to further increase the sensitivity of the mixed EWMA-CUSUM chart, Riaz et al. [8] suggested an AIB mixed version of the EWMA-CUSUM mean chart. Similarly, Aslam et al. [9] introduced mixed control chart for attribute data. Likewise, Aslam [10] suggested mixed EWMA-CUSUM and mixed accelerated hybrid censored control chart for Weibull distribution. Also, Aslam et al. [11] suggested mixed chart using EWMA statistic. On similar lines, Haq and Bibi [12] suggested the dual CUSUM charts with the help of auxiliary information to improve the process mean monitoring. Similarly, Anwar et al. [13] suggested AIB-mixed EWMA-CUSUM and AIB-mixed CUSUM-EWMA charts for efficient monitoring of process location. Also, Anwar et al. [14] proposed an AIB-modified EWMA chart for improved process location monitoring. Anwar et al. (2021a) suggested an AIB double homogeneously weighted moving average control chart for the process mean on the same lines. It has been found that these charts are superior to the non-AIB-based chart for detecting various process mean shifts. For more related works, we refer to Aslam et al. [15], Lee [16], Abid et al. [17], Khan et al. [18], Haq et al. [19], Hussain et al. [20], Hussain et al. [20], Anwar et al. [21], and the references cited therein.

Existing control charts such as CUSUM, AIB-CUSUM, EWMA, and AIB-EWMA charts are designed to detect a particular shift level efficiently by selecting an appropriate reference value. However, the shift size is rarely known and can only be assumed to fall within a certain range. The charts with reference values designed for a prespecified shift usually do not perform well for the whole shift range. Hence, it is important to design a control chart for detecting a range of known or unknown shift levels. Because we rarely know the exact shift size before it is detected, several techniques have been developed to handle the issue of detecting unknown shifts within a certain range. For example, Zhao et al. [22] proposed a method by combining two different CUSUM charts, namely, the dual CUSUM (DC) charts which are used to detect a range of shifts. Hany and Mahmoud [23] provided Crosier CUSUM (CC) control chart that performs better than the classical CUSUM chart. Similarly, Haq and Munir [24] suggested proposed CC and Shewhart-CUSUM (SC) charts for the process mean under ranked set sampling (RSS) scheme. Moreover, the false initial response features were attached to improve the control chart's detection ability. The RSS-based CC and SC charts are very efficient for monitoring small and large shifts in the process mean compared to the existing counterparts based on a simple random sampling scheme. Later, Abbas et al. [25] suggested a new charting scheme called mixed EWMA dual-CUSUM (EDC) chart to monitor the process mean. The EDC chart provided a good overall detection over the DC and dual-Crosier CUSUM (DCC) charts when detecting a range of mean shift sizes. After that, Song et al. [26] presented an efficient approach of designing distribution-free exponentially weighted moving average schemes with dynamic fast initial response for joint monitoring of location and scale.

Furthermore, Saha et al. [27] advocated two CUSUM schemes for simultaneous monitoring of unknown parameters of a shifted exponential process and its application in monitoring of call durations in telemarketing. Afterward, Haq and Syed [28] recently introduced CUSUM and dual CUSUM charts for the enhanced process mean monitoring. Also, Haridy et al. [29] instigated an improved design of exponentially weighted moving average scheme for monitoring attributes. For more related works, readers can refer to Raji et al. [30], Haq and Bibi [31], Haq and Bibi [31], Javaid et al. [32], Aslam and Anwar [33], Rasheed, et al. [34], and the references therein.

As mentioned before that the CC, EDC, and DCC charts are very efficient for the detection of different shift sizes when the process parameters are univariate and free from any extra information like auxiliary information. Sometimes, the practitioners are interested in monitoring processes where the quality characteristic is accessed along with auxiliary information variables. In this case, the CC, EDC, and DCC charts are inefficient. Moreover, the performance of the EDC chart is better than CC and DCC charts. Taking motivation from these facts, we propose an EWMA-DCC chart, called EDCC chart, for monitoring variations in the process mean, considering shifts lying within an interval. In addition, by using the AIB mean estimator, we propose AIB-based EDC (AIB-EDC) and AIB-based EDCC (AIB-EDCC) charts for efficiently monitoring the process mean shifts within an interval. The performance of the proposed charts is evaluated with the help of the average run length (ARL), the standard deviation of run-length (SDRL) and median run length (MRL), extraquadratic loss (EQL), and integral relative ARL (IRARL). The findings revealed that the proposed AIB-EDC and AIB-EDCC charts are more sensitive in detecting process mean shifts than their competitors used in this study. The proposed AIB-EDC and AIB-EDCC charts also outperform in terms of overall performance. A similar trend is observed when these benchmark CUSUM charts are compared with the proposed charts with FIR features.

The remainder of this paper is organized as follows. In Section 2, the DC, DCC, and EDC charts are presented. Section 3 presents the details of the proposed EDCC, AIB-EDCC, and AIB-EDC charts with and without FIR features. Then, the RL performance of different control charts and some design guidelines of the charts are provided in Section 4. Section 5 contains a real data example to illustrate the application of our proposed charts. Some conclusions and discussions are given in Section 6.

2. Existing CUSUM Charts

In this section, a brief review of some existing CUSUM location charts is provided. Let us assume $X_{t,1}, \dots, X_{t,n}$, $t = 1, 2, \dots$, represents a sample of size $n \geq 1$ from normally distributed quality characteristics having mean μ_0 and standard deviation σ_0 , i.e., $X_t \sim N(\mu_0 + \delta\sigma_0, \sigma_0)$, where δ represents the shift in the process mean level. The process stays in control if $\delta = 0$ and considered out-of-control for $\delta \neq 0$. Also, $\bar{X}_t = \sum_{j=1}^n X_{t,j}$ is the sample mean and $\mu_{\bar{X}_t} = \mu_0 + \delta\sigma_0$ and $\sigma_{\bar{X}_t} = \sigma_0/\sqrt{n}$, respectively. Without loss of

generality, the process mean μ_0 and σ_0 are assumed to be 0 and 1, respectively, and the sample size $n = 1$.

2.1. Classical CUSUM Chart. The usual CUSUM \bar{X} chart is defined as

$$\begin{cases} C_t^+ = \max [0, +(\bar{X}_t - \mu_0) - K + C_{t-1}^+] \\ C_t^- = \max [0, -(\bar{X}_t - \mu_0) - K + C_{t-1}^-] \end{cases}, \quad (1)$$

where K ($K = k\delta/\sqrt{n}$) is the reference value. An out-of-control signal is detected when C_t^+ (for the upper-sided chart) or C_t^- (for the lower-sided chart) exceeds the decision interval h , where h is determined to obtain a desired in-control ARL. When the mean shift size δ is known, it has become well known that the upper-sided or lower-sided CUSUM \bar{X} chart can be optimally designed using $K = \delta/2$.

2.2. DC Chart. Zhao et al. [22] suggested using DC chart to detect different levels of mean shift. The DC chart outperforms the CUSUM chart when detecting mean shifts in different ranges. The chart consists of plotting two upper ($A_{1,t}^+, A_{1,t}^-$) and two lower ($A_{2,t}^+, A_{2,t}^-$) CUSUM statistics, respectively, based on the sample mean \bar{X}_t at time, given by

$$\begin{cases} A_{1,t}^+ = \max [0, +(\bar{X}_t - \mu_0) - k_1 + A_{1,t-1}^+] \\ A_{1,t}^- = \max [0, -(\bar{X}_t - \mu_0) - k_1 + A_{1,t-1}^-] \end{cases}, \quad (2)$$

$$\begin{cases} A_{2,t}^+ = \max [0, +(\bar{X}_t - \mu_0) - k_2 + A_{2,t-1}^+] \\ A_{2,t}^- = \max [0, -(\bar{X}_t - \mu_0) - k_2 + A_{2,t-1}^-] \end{cases}, \quad (3)$$

where $A_{i,0}^+ = A_{i,0}^- = 0$ and k_i are the reference parameters for $i = 1, 2$.

The two-sided DC chart gives an out-of-control signal whenever $A_{i,t}^+ > h_i$ or $A_{i,t}^- > h_i$, for $i = 1, 2$. The values of h_i are selected so that the in-control ARL of the DC chart reaches the desired level. On similar lines, the one-sided DC chart triggers an out-of-control signal whenever only $A_{i,t}^+ > h_i$ for the upper-sided chart to detect an upward shift or $A_{i,t}^- > h_i$ for the lower-sided chart to detect a downward shift in the process mean, respectively. In order to increase the sensitivities of the DC chart against the initial process shifts, it is possible to incorporate the FIR features into this chart. On the lines of Lucas and Crosier [35], the FIR features are applied to the DC chart by modifying $A_{i,0}^+ = A_{i,0}^- = h_i/2$ for $i = 1, 2$.

As our interest lies in detecting shifts that are expected to lie with an interval, for all the control charts studied in this paper, we consider $k_1 = (3a + b)/8$ and $k_2 = (a + 3b)/8$ with $k_1 h_1 = k_2 h_2$ and $k_1 + h_1 > k_2 + h_2$, which were also recommended by Zhao et al. [22].

2.3. EDC Chart. Abbas et al. [25] proposed a more sensitive EDC control chart for detecting small shifts in the process mean. Similar to the DC chart, the plotting statistics ($E_{1,t}^+, E_{2,t}^+$) (upper-sided) and ($E_{1,t}^-, E_{2,t}^-$) (lower-sided) of the EDC chart is

$$\begin{cases} E_{1,t}^+ = \max [0, +(M_t - \mu_0) - k_1 + E_{1,t-1}^+] \\ E_{1,t}^- = \max [0, -(M_t - \mu_0) - k_1 + E_{1,t-1}^-] \end{cases}, \quad (4)$$

$$\begin{cases} E_{2,t}^+ = \max [0, +(M_t - \mu_0) - k_2 + E_{2,t-1}^+] \\ E_{2,t}^- = \max [0, -(M_t - \mu_0) - k_2 + E_{2,t-1}^-] \end{cases}, \quad (5)$$

where

$$M_t = \lambda \bar{X}_t + (1 - \lambda)M_{t-1}. \quad (6)$$

Now, the mean and variance of statistic are given as

$$E(M_t) = \mu_{\bar{X}_t},$$

$$\text{Var}(M_t) = \sigma_{\bar{X}_t}^2 \left(\frac{\lambda}{(2 - \lambda)} (1 - (1 - \lambda)^{2t}) \right), \quad (7)$$

where $\lambda \in (0, 1]$ is the smoothing parameter, $E_{i,0}^+ = E_{i,0}^- = 0$, $i = 1, 2$, and k_i are the reference parameter. With the time t getting large, the factor $(1 - (1 - \lambda)^{2t})$ tends to unity, and ultimately, the variance of M_t converges to $\sigma_{\bar{X}_t}^2 \lambda / (2 - \lambda)$.

The EDC chart plots $E_{i,t}^+$ and $E_{i,t}^-$ against h_i and the value of h_i are selected to match the in-control ARL of the EDC chart to the desired level. If both $E_{i,t}^+$ and $E_{i,t}^-$ are less than h_i , it is stated that the process is in an in-control state. The two-sided EDC chart issues an out-of-control signal whenever $E_{i,t}^+$ or $E_{i,t}^-$ exceeds h_i . The one-sided EDC chart works with only the charting statistic $E_{i,t}^+$ or $E_{i,t}^-$. If $E_{i,t}^+$ exceeds h_i , the upper-sided EDC triggers an out-of-control signal. If $E_{i,t}^-$ exceeds h_i , the lower-sided EDC triggers an out-of-control signal. For more details on the EDC chart, readers can refer to Abbas et al. [25]. Similar to the FIR-DC chart, the FIR-EDC chart with the 50% head start $E_{i,0}^+ = E_{i,0}^- = h_i/2$, for $i = 1, 2$, are also suggested to protect the initial problems.

2.4. DCC Chart. The CC chart has been suggested by Crosier [36] for monitoring the process mean. The CC chart is more sensitive than the classical DC chart. Using the sequence \bar{X}_t , the plotting-statistic of the DCC mean chart is given as follows:

$$\begin{cases} D_{1,t} = 0 & \text{if } C_{1,t} \leq k_1, \\ (\bar{X}_t - \mu_0 + D_{1,t-1})(1 - k_1/C_{1,t}) & \text{if } C_{1,t} > k_1, \end{cases} \quad (8)$$

$$\begin{cases} D_{2,t} = 0 & \text{if } C_{2,t} \leq k_2, \\ (\bar{X}_t - \mu_0 + D_{2,t-1})(1 - k_2/C_{2,t}) & \text{if } C_{2,t} > k_2, \end{cases} \quad (9)$$

where $C_{i,t} = |\bar{X}_t - \mu_0 + D_{i,t-1}|$ with $D_{i,0} = 0$ for $i = 1, 2$. Here, $k_i > 0$ with $i = 1, 2$ are the reference parameters of the DCC chart. The DCC chart works with two different plotting statistics, $D_{1,t}$ and $D_{2,t}$. An out-of-control signal is initiated by the two-sided DCC chart whenever $D_{i,t} > h_i$ or $D_{i,t} < -h_i$, where h_i , $i = 1, 2$ are the decision intervals. For the one-sided charts, the upper-sided chart triggers an out-of-control signal when $D_{i,t} > h_i$ and the lower-sided chart gives an out-of-control signal when $D_{i,t} < -h_i$. In addition, with fixed k_1 and k_2 for a given mean shift interval, the values of either h_1 or h_2 are determined to get the desired in-control ARL for

the DCC chart. To increase the sensitivities of the DCC chart, the FIR feature is applied by adjusting the DCC chart with the 50% head start to protect the initial problems, i.e., $D_{i,0}^+ = D_{i,0}^- = h_i/2$, for $i = 1, 2$, called as FIR-DCC chart.

3. Proposed Control Chart

This section proposes three new CUSUM control charts to efficiently monitor a wide range of shifts in the process mean level. These include an EWMA-DCC (EDCC) chart, the auxiliary information-based EDC (AIB-EDC) chart, and the auxiliary information-based EDCC (AIB-EDCC) chart. Both the one-sided and two-sided versions of these charts are described as follows.

3.1. EDCC Chart. In order to enhance the detection ability of the DCC chart, the mixture charting structure of EWMA with DCC charts are integrated into a single control chart. The plotting statistics of two CUSUM statistics, say $G_{1,t}$ and $G_{2,t}$, based on M_t , are given by

$$G_{1,t} \begin{cases} 0 & \text{if } C_{1,t} \leq k_1, \\ (M_t - \mu_0 + G_{1,t-1})(1 - k_1/C_{1,t}) & \text{if } C_{1,t} > k_1, \end{cases} \quad (10)$$

$$G_{2,t} \begin{cases} 0 & \text{if } C_{2,t} \leq k_2, \\ (M_t - \mu_0 + G_{2,t-1})(1 - k_2/C_{2,t}) & \text{if } C_{2,t} > k_2, \end{cases} \quad (11)$$

where $C_{i,t} = |M_t - \mu_0 + G_{i,t-1}|$ with $G_{i,0} = 0$ for $i = 1, 2$ and M_t is defined in (11). Here, k_i , $i = 1, 2$, are the reference values of the EDCC chart. The EDCC chart works with two different plotting statistics, i.e., $G_{1,t}$ and $G_{2,t}$. An out-of-control signal is initiated by the two-sided EDCC chart whenever $G_{i,t} > h_i$ or $G_{i,t} < -h_i$, where h_i , $i = 1, 2$ are the decision intervals. For the one-sided charts, the upper-sided chart triggers an out-of-control signal when $G_{i,t} > h_i$ and the lower-sided chart gives an out-of-control signal when $G_{i,t} < -h_i$. The values of h_i are selected so that the in-control ARL of the EDCC chart reaches the desired level. For the EDCC chart, an FIR feature is attached to guard against the initial/startup problems, i.e., $G_{i,0} = h_i/2$, for $i = 1, 2$. This FIR feature enables the EDCC chart to respond to an off-target process at the startup quickly.

3.2. AIB-EDC Chart. Suppose there exists an auxiliary characteristic Y which is correlated with the quality characteristic of interest X . The observations of X and Y are obtained in paired form, i.e., (X_t, Y_t) for $t \geq 1$, from the bivariate normal distribution, i.e., $(X_t, Y_t) \sim N_2(\mu_X, \mu_Y, \sigma_X^2, \sigma_Y^2, \rho)$ with (μ_X, μ_Y) representing the means, (σ_X^2, σ_Y^2) representing the variances and ρ is a correlation coefficient between X and Y . A bivariate random sample of size n is taken from the process (X_t, Y_t) at the time t , denoted by (X_{tj}, Y_{tj}) , for $t = 1, 2, \dots$. Let $\bar{Y}_t = (1/n) \sum_{j=1}^n Y_{tj}$, denotes the sample mean of the auxiliary characteristic Y . Using these notations, the regression estimator of the process mean is given by (cf. Riaz [37] and Abbas et al. [4]):

$$Q_t = \bar{X}_t + \rho \left(\frac{\sigma_X}{\sigma_Y} \right) (\mu_Y - \bar{Y}_t). \quad (12)$$

The mean and variance of the statistic Q_t in (13) are given as

$$E(Q_t) = \mu_{\bar{X}_t}, \quad (13)$$

$$Var(Q_t) = \sigma_{\bar{X}_t}^2 (1 - \rho^2). \quad (14)$$

(13) and (14) imply that Q_t is also an unbiased estimator of $\mu_{\bar{X}_t}$ and $\sigma_{Q_t}^2 < \sigma_{\bar{X}_t}^2$.

Using the sequence Q_t based on the regression estimator in (12), the upper $(E_{1,t}^+, E_{2,t}^+)$ and two lower $(E_{1,t}^-, E_{2,t}^-)$ plotting statistics of the AIB-EDC mean chart are given by

$$\begin{cases} E_{1,t}^+ = \max [0, +(M_t - \mu_0) - k_1 + E_{1,t-1}^+] \\ E_{1,t}^- = \max [0, -(M_t - \mu_0) - k_1 + E_{1,t-1}^-] \end{cases}, \quad (15)$$

$$\begin{cases} E_{2,t}^+ = \max [0, +(M_t - \mu_0) - k_2 + E_{2,t-1}^+] \\ E_{2,t}^- = \max [0, -(M_t - \mu_0) - k_2 + E_{2,t-1}^-] \end{cases}, \quad (16)$$

where $E_{i,0}^+ = E_{i,0}^- = 0$ with $i = 1, 2$. k_i and h_i are the reference parameters and decision intervals, respectively, of the AIB-EDC chart. The value of h_i is selected to obtain the in-control ARL of the AIB-EDC chart at a desired level. The two-sided and one-sided AIB-EDC charts work similarly to EDC charts presented in Section 2.3.

The statistic M_t in (15) and (16) is defined as,

$$M_t = \lambda Q_t + (1 - \lambda)M_{t-1}, \quad (17)$$

where $\lambda \in (0, 1]$. Now the mean and variance of M_t are given as:

$$E(M_t) = \mu_{Q_t}, \quad (18)$$

$$Var(M_t) = \sigma_{Q_t}^2 \left(\frac{\lambda}{(2 - \lambda)} (1 - (1 - \lambda)^{2t}) \right).$$

With the time t increasing, the factor $(1 - (1 - \lambda)^{2t})$ tends to unity, and ultimately the variance of M_t will converge to $\sigma_{Q_t}^2 \lambda / (2 - \lambda)$. An FIR feature with the AIB-EDC chart to increase its sensitivity against the initial problems or shifts in the process mean, called the FIR-AIB-EDC chart, is also suggested. The FIR-AIB-EDC chart is suggested with the 50% head start, i.e. $E_{i,0}^+ = E_{i,0}^- = h_i/2$ for $i = 1, 2$.

3.3. AIB-EDCC Chart. The auxiliary information based EDCC, namely the AIB-EDCC chart, is based on two plotting statistics $(G_{1,t}$ and $G_{2,t})$, defined below:

$$G_{1,t} = \begin{cases} 0 & \text{if } C_{1,t} \leq k_1, \\ (M_t - \mu_0 + G_{1,t-1})(1 - k_1/C_{1,t}) & \text{if } C_{1,t} > k_1, \end{cases} \quad (19)$$

$$G_{2,t} = \begin{cases} 0 & \text{if } C_{2,t} \leq k_2, \\ (M_t - \mu_0 + G_{2,t-1})(1 - k_2/C_{1,t}) & \text{if } C_{2,t} > k_2, \end{cases} \quad (20)$$

where $C_{i,t} = |M_t - \mu_0 + G_{i,t-1}|$ with $G_{i,0} = 0$ for $i = 1, 2$ and M_t is defined in (17). k_i represents the reference value and h_i is the decision interval. The two-sided and one-sided AIB-EDCC charts work similarly to the EDCC charts presented in Section 3.1. An FIR feature can also be attached to the AIB-EDCC chart by setting $G_{i,0} = h_i/2$ for $i = 1, 2$, called the FIR-AIB-EDCC chart.

4. Performance Comparison

A detailed comparative study of the proposed control chart with some of the existing control charts is provided in this section.

The performance of a control chart is generally evaluated in terms of its run length properties, including the ARL, MRL and SDRL. These measures are used to evaluate the sensitivity of a control chart for a specific shift. For an in-control process, the in-control ARL (ARL_0) should be large enough to avoid frequent false alarms. While for an out-of-control process, the out-of-control ARL (ARL_1) should be as small as possible to detect the out-of-control signals quickly. The same implies to the MRL and SDRL. The smaller the SDRL of a control chart for a given shift, the better performance of a control chart at a specific shift will be. Many approaches are frequently used to approximate the run length characteristics of a control chart, including the integral equations, Markov chain, and the Monte Carlo simulation. In this paper, the Monte Carlo simulation method is used to obtain estimates of the run length characteristics due to the complexity of the charting statistics.

In order to study the overall performance of a control chart for a range of shift sizes, an alternative performance measure IRARL that describes the effectiveness of a control chart over the whole process shift domain ($a \leq \delta \leq b$) is considered in our study to investigate the run length performance of the control charts, see Zhao et al. [22] and Wu et al. [38]. The IRARL can be formulated as follows:

$$IRARL = E \left[\frac{ARL_c(\delta)}{ARL_{opt}(\delta)} \right] = \int \left[\frac{ARL_c(\delta)}{ARL_{opt}(\delta)} \right] dF(\delta). \quad (21)$$

Here, the traditional optimal one-sided CUSUM \bar{X} chart is considered as the benchmark control chart for a specific shift. Also, the $ARL_c(\delta)$ represents the ARL_1 of the compared control chart under the mean shift δ and $ARL_{opt}(\delta)$ can be defined as the ARL_1 of the traditional CUSUM \bar{X} chart in Section 2.1 with $k = \delta/2$ for various values of δ in the range $[a, b]$. In addition, $F(\delta)$ is the cumulative distribution function (CDF) of shift δ . In practice, if we have no prior information about the mean shift, the CDF of uniform distribution $U[a, b]$ can be used, see Zhao et al. [22] and Tanaka et al. [39]. IRARL values are obtained by applying the Simpsons method using the integral function available in R “Bolstad” statistical package.

In what follows, all the simulation results are done with $ARL_0 = 300$. For simplicity, different size of ranges $[0.25, 1]$, $[0.25, 3]$, $[0.25, 5]$, $[1, 3]$, and $[1, 5]$ are considered for the out-of-control situations. On similar lines with Abbas

et al. [25], the values of smoothing parameter $\lambda = 0.05, 0.25,$ and 0.50 are selected in the EWMA statistic. For the AIB-based charts, ρ is set as 0.5 and 0.75 for discussion (see Anwar et al. [14]).

Based on 10^5 replications under each simulation, these control charts’ run length characteristics are computed and reported in Tables 1–3. The main findings are listed in the following points.

As might be anticipated that, having fixed the ARL_0 , the out-of-control ARL/MRL/SDRL of the proposed charts decrease as a function of δ , i.e., as the value of δ increases, the out-of-control ARL/MRL/SDRL tends to decrease and vice versa. For example, in Table 1, when $\lambda = 0.5$, the ARL/MRL/SDRL values of the AIB-EDCC chart decrease from $44.37/35.00/32.58$ down to $7.90/7.00/2.69$ with δ increasing from 0.25 up to 1 . Overall, the proposed one-sided EDC and EDCC charts with AIB outperform the exiting control charts for different shifts. For example, from Table 1, it can be noted that when $\lambda = 0.5$, the IRARL is 0.86 for the AIB-EDC and AIB-EDCC charts, which are both smaller than the IRARL values of the DC (1.04), DCC (0.96), and EDC (1.03) charts. On the other hand, the AIB-EDCC control chart is very efficient than the AIB-EDC chart for a larger value of ρ . For example, at $\delta = 0.25$ and $\rho = 0.75$, the ARL value AIB-EDC chart is 33.26 , whereas the ARL value AIB-EDCC chart is 33.15 .

From Table 2, at $\lambda = 0.5$, when δ increasing from 0.25 up to 3 , the ARL/MRL/SDRL of AIB-EDCC chart also decreases from $70.69/54/58.01$ down to $2.30/2/0.5$. Likewise, the ARL values of the AIB-EDC and AIB-EDCC control charts decrease with the increase of ρ from 0.50 to 0.75 . For example, at $\delta = 0.53$ and $\rho = 0.50$, the ARL values AIB-EDC and AIB-EDCC charts are 18.15 and 18.17 , whereas the ARL values at $\delta = 0.53$ and $\rho = 0.75$ are 13.60 and 13.64 , respectively (see Table 2).

In addition, it can also be noted that the EDC and EDCC charts without and with AIB outperform the DC and DCC charts for a specific small shift in the shift ranges. For example, when $\delta = 0.25$ in Table 3, the ARL = $45.50, 45.58, 31.81,$ and 38.97 of the EDC, EDCC, AIB-EDC, and AIB-EDCC charts are all smaller than the ARL = 91.95 and 88.98 of the DC and DCC charts. Interestingly, that the proposed AIB-EDC and AIB-EDCC charts outperform the DC, EDC, OC, EDC, and EDCC charts even for large λ . For example, when $\delta = 0.25$, the ARL values of DC, EDC, OC, EDC, EDCC, AIB-EDC ($\lambda = 0.75$), and AIB-EDCC ($\lambda = 0.75$) are $91.59, 88.98, 52.31, 45.50, 35.22,$ and 35.26 , respectively (see Table 3).

From Table 4, when δ increasing from 1 up to 3 at $\lambda = 0.5$, the ARL/MRL/SDRL values of the AIB-EDCC decrease from $6.45/6/3.09$ to $1.91/2/0.51$. Likewise, for the overall performance measures of the control charts, the proposed AIB-EDC and AIB-EDCC charts have minimum values of EQL, i.e., 8.77 and 8.77 , respectively. This implies that the proposed AIB-EDC and AIB-EDCC charts are more efficient in terms of overall performance measures (see Table 4). Furthermore, the proposed charts are also presented at another range of 1 to 5 . From Table 5, when $\lambda = 0.5$, the AIB-EDCC ARL/MRL/SDRL values decrease from

TABLE 2: The ARL_1 profile of the one-sided EDC and EDCC charts when $\delta \in [0.25, 3]$ with $ARL_0 = 300$.

δ	DC	DCC	EDC	EDCC	$\lambda = 0.05$				$\lambda = 0.50$				$\lambda = 0.50$				OC
					$\rho = 0.50$		$\rho = 0.75$		$\rho = 0.50$		$\rho = 0.75$		$\rho = 0.50$		$\rho = 0.75$		
					AIB-EDC	AIB-EDCC	AIB-EDC	AIB-EDCC	AIB-EDC	AIB-EDCC	AIB-EDC	AIB-EDCC	AIB-EDC	AIB-EDCC	AIB-EDC	AIB-EDCC	
h_1	4.7347	4.5605	23.018	23.150	23.018	23.150	20.200	20.233	20.200	20.233	11.599	11.60	11.599	11.60	11.599	11.60	$k = \delta/2$
h_2	1.9184	1.8478	9.3263	9.3797	9.3263	9.3797	8.1845	8.1979	8.1845	8.1979	4.6996	4.70	4.6996	4.70	4.6996	4.70	52.31
0.25	ARL	80.04	78.80	46.77	46.90	30.37	30.42	61.30	61.30	41.46	41.67	89.27	88.80	70.52	70.69	45.09	45.22
	MRL	57.00	56.00	39.00	39.00	27.00	27.00	50.00	50.00	35.00	36.00	67.00	66.00	54.00	54.00	36.00	36.00
	SDRL	75.48	74.59	30.03	30.10	24.13	24.34	43.66	43.66	26.05	26.13	76.07	76.03	57.50	58.01	33.25	33.17
0.53	ARL	25.27	24.52	21.15	21.25	18.15	18.17	13.60	13.64	13.64	14.69	26.06	26.10	20.88	20.94	13.97	13.97
	MRL	20.00	19.00	19.00	19.00	17.00	17.00	13.00	13.00	13.00	13.00	22.00	22.00	18.00	19.00	13.00	13.00
	SDRL	20.34	19.87	9.81	9.88	7.99	7.99	5.23	5.24	5.24	6.72	16.17	16.13	12.10	12.05	7.19	7.23
0.80	ARL	12.40	12.06	13.63	13.67	11.74	11.77	8.97	9.01	14.73	14.74	12.15	12.18	11.00	11.37	7.70	7.68
	MRL	11.00	10.00	13.00	13.00	11.00	11.00	9.00	9.00	13.00	13.00	11.00	11.00	11.00	11.00	7.00	7.00
	SDRL	8.22	8.09	5.28	5.26	4.16	4.17	2.67	2.68	6.74	6.79	5.21	5.25	5.60	5.57	3.50	3.49
1.08	ARL	7.66	7.40	10.02	10.04	8.70	8.72	6.77	6.78	9.97	9.94	8.38	8.39	7.36	7.38	5.08	5.09
	MRL	7.00	7.00	9.00	9.00	8.00	8.00	7.00	7.00	9.00	9.00	8.00	8.00	7.00	7.00	5.00	5.00
	SDRL	4.41	4.33	3.22	3.22	2.54	2.53	1.67	1.66	3.85	3.82	2.88	2.87	3.29	3.32	1.92	1.91
1.35	ARL	5.42	5.23	8.08	8.11	7.06	7.08	5.55	5.56	7.66	7.65	6.57	6.57	5.40	5.41	3.89	3.89
	MRL	5.00	5.00	8.00	8.00	7.00	7.00	6.00	6.00	7.00	7.00	6.00	6.00	5.00	5.00	4.00	4.00
	SDRL	2.94	2.87	2.24	2.23	1.78	1.78	1.19	1.19	2.46	2.44	1.84	1.84	2.11	2.11	1.21	1.21
1.63	ARL	4.05	3.91	6.77	6.80	5.96	5.96	4.71	4.72	6.28	6.28	5.47	5.46	4.27	4.25	3.18	3.18
	MRL	4.00	4.00	7.00	7.00	6.00	6.00	5.00	5.00	6.00	6.00	5.00	5.00	4.00	4.00	3.00	3.00
	SDRL	2.12	2.08	1.66	1.67	1.34	1.34	0.91	0.91	1.70	1.70	1.32	1.32	1.93	1.91	0.86	0.86
1.90	ARL	3.20	3.10	5.90	5.92	5.20	5.22	4.13	4.14	5.40	5.41	4.73	4.73	3.73	3.74	2.73	2.73
	MRL	3.00	3.00	6.00	6.00	5.00	5.00	4.00	4.00	5.00	5.00	4.00	4.00	3.00	3.00	2.00	2.00
	SDRL	1.64	1.60	1.32	1.32	1.07	1.07	0.74	0.75	1.30	1.30	1.03	1.03	1.39	1.39	0.68	0.68
2.18	ARL	2.59	2.51	5.23	5.25	4.63	4.64	3.69	3.70	4.76	4.77	4.19	4.19	3.33	3.33	2.41	2.41
	MRL	2.00	2.00	5.00	5.00	4.00	4.00	3.00	3.00	4.00	4.00	3.00	3.00	2.00	2.00	1.50	1.50
	SDRL	1.28	1.25	1.08	1.08	0.88	0.88	0.64	0.64	1.04	1.04	0.85	0.84	0.58	0.58	0.43	0.43
2.45	ARL	2.17	2.12	4.73	4.74	4.00	4.20	3.34	3.35	4.29	4.29	3.78	3.79	3.05	3.05	2.18	2.18
	MRL	2.00	2.00	5.00	5.00	4.00	4.00	3.00	3.00	4.00	4.00	3.00	3.00	2.00	2.00	1.50	1.50
	SDRL	1.02	1.01	0.91	0.92	0.76	0.75	0.54	0.54	0.87	0.88	0.72	0.72	0.49	0.49	0.34	0.34
2.73	ARL	1.87	1.82	4.32	4.33	3.82	3.84	3.08	3.09	3.90	3.91	3.46	3.46	2.81	2.81	2.03	2.03
	MRL	2.00	2.00	4.00	4.00	3.00	3.00	2.00	2.00	3.00	3.00	2.00	2.00	1.50	1.50	1.00	1.00
	SDRL	0.83	0.82	0.79	0.79	0.67	0.67	0.44	0.44	0.75	0.75	0.62	0.62	0.48	0.48	0.34	0.34
3.00	ARL	1.64	1.60	3.99	4.00	3.53	3.54	2.89	2.90	3.60	3.60	3.21	3.21	2.58	2.58	1.93	1.93
	MRL	2.00	2.00	4.00	4.00	3.00	3.00	2.00	2.00	3.00	3.00	2.00	2.00	1.50	1.50	1.00	1.00
	SDRL	0.70	0.69	0.71	0.71	0.60	0.60	0.43	0.42	0.66	0.66	0.54	0.53	0.51	0.51	0.33	0.33
EQL	10.47	10.17	18.60	18.66	16.27	16.42	13.08	13.08	14.09	14.12	12.28	12.28	9.70	9.57	9.99	10.01	7.63
IRARL	1.12	1.09	1.75	1.76	1.53	1.54	1.22	1.22	1.36	1.36	1.18	1.18	0.92	0.91	0.99	0.74	1.00

TABLE 7: The ARL_1 profile of the two-sided EDC and EDCC charts when $\delta \in [0.25, 5]$ with $ARL_0 = 300$.

δ	h_1	h_2	$\lambda = 0.05$												$k = \delta/2$																
			$\rho = 0.50$				$\rho = 0.75$				$\rho = 0.50$					$\rho = 0.75$															
			DC	DCC	EDC	EDCC	AIB-EDC	AIB-EDCC	EDC	EDCC	AIB-EDC	AIB-EDCC	EDC	EDCC		AIB-EDC	AIB-EDCC	EDC	EDCC	AIB-EDC	AIB-EDCC										
0.25	MRL	101.00	100.00	54.00	53.00	40.63	39.40	40.63	31.46	31.46	19.35	19.39	62.85	62.58	48.56	48.06	28.70	28.70	31.00	31.00	66.00	65.00	54.00	53.00	35.00	35.00	43.00	43.00	52.31	52.31	
0.73	MRL	16.00	15.00	20.00	20.00	17.68	17.62	13.18	13.16	15.41	15.26	12.88	12.74	9.43	9.36	15.03	14.74	11.96	11.85	11.85	11.85	11.85	11.85	11.96	11.96	11.85	11.85	8.04	8.04	13.03	13.03
1.20	MRL	7.50	7.32	12.03	11.99	6.82	6.79	5.68	5.68	5.70	5.70	5.70	5.70	5.70	5.70	5.70	5.70	5.70	5.70	5.70	5.70	5.70	5.70	5.70	5.70	5.70	5.70	5.70	5.70	5.70	5.70
1.68	MRL	4.00	4.00	8.00	8.00	4.00	4.00	4.00	4.00	4.00	4.00	4.00	4.00	4.00	4.00	4.00	4.00	4.00	4.00	4.00	4.00	4.00	4.00	4.00	4.00	4.00	4.00	4.00	4.00	4.00	4.00
2.15	MRL	3.00	3.00	6.00	6.00	3.00	3.00	3.00	3.00	3.00	3.00	3.00	3.00	3.00	3.00	3.00	3.00	3.00	3.00	3.00	3.00	3.00	3.00	3.00	3.00	3.00	3.00	3.00	3.00	3.00	3.00
2.63	MRL	2.00	2.00	5.00	5.00	2.00	2.00	2.00	2.00	2.00	2.00	2.00	2.00	2.00	2.00	2.00	2.00	2.00	2.00	2.00	2.00	2.00	2.00	2.00	2.00	2.00	2.00	2.00	2.00	2.00	2.00
3.10	MRL	2.00	2.00	4.00	4.00	2.00	2.00	2.00	2.00	2.00	2.00	2.00	2.00	2.00	2.00	2.00	2.00	2.00	2.00	2.00	2.00	2.00	2.00	2.00	2.00	2.00	2.00	2.00	2.00	2.00	2.00
3.58	MRL	1.00	1.00	4.00	4.00	1.00	1.00	1.00	1.00	1.00	1.00	1.00	1.00	1.00	1.00	1.00	1.00	1.00	1.00	1.00	1.00	1.00	1.00	1.00	1.00	1.00	1.00	1.00	1.00	1.00	1.00
4.05	MRL	1.00	1.00	4.00	4.00	1.00	1.00	1.00	1.00	1.00	1.00	1.00	1.00	1.00	1.00	1.00	1.00	1.00	1.00	1.00	1.00	1.00	1.00	1.00	1.00	1.00	1.00	1.00	1.00	1.00	1.00
4.53	MRL	1.00	1.00	4.00	4.00	1.00	1.00	1.00	1.00	1.00	1.00	1.00	1.00	1.00	1.00	1.00	1.00	1.00	1.00	1.00	1.00	1.00	1.00	1.00	1.00	1.00	1.00	1.00	1.00	1.00	1.00
5.00	MRL	1.00	1.00	4.00	4.00	1.00	1.00	1.00	1.00	1.00	1.00	1.00	1.00	1.00	1.00	1.00	1.00	1.00	1.00	1.00	1.00	1.00	1.00	1.00	1.00	1.00	1.00	1.00	1.00	1.00	1.00
EQL	SDRL	15.95	15.73	38.48	38.32	33.97	33.82	26.25	26.12	24.96	24.77	21.83	21.70	16.14	16.01	19.26	18.99	16.14	15.94	15.94	15.94	15.94	16.14	16.14	16.14	16.14	12.32	12.25	13.49	13.49	13.49
IRARL	SDRL	1.33	1.31	2.59	2.58	2.27	2.26	1.76	1.75	1.75	1.73	1.51	1.50	1.12	1.11	1.43	1.41	1.19	1.18	1.18	1.18	1.19	1.19	1.19	1.19	0.88	0.87	1.00	1.00	1.00	

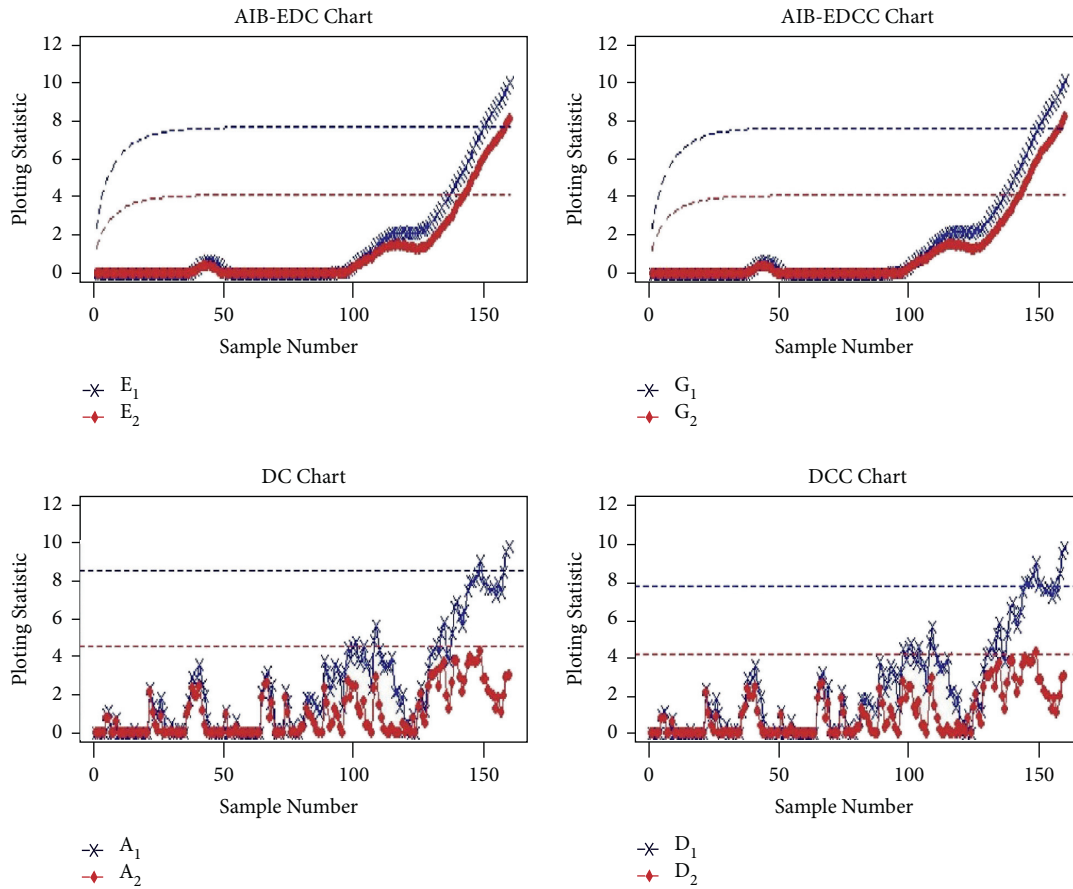


FIGURE 1: The dual and mixed dual process mean charts for the film thickness dataset.

6.29/5/3.35 down to 1.02/1/0.16. For the monitoring of large shifts, the AIB-EDCC chart is better for a larger value of λ . For example, at $\lambda = 0.05, 0.25, 0.50$, the AIB-EDCC chart (with $\rho = 0.75$ and $\delta = 1$) provides ARL of 5.91, 5.09, and 4.37, respectively (see Table 5).

It can be noted that, from Table 6, the FIR AIB-EDC and ABI-EDCC charts are better than other FIR charts in the detection of a whole range of shifts. For example, when $\lambda = 0.5$, the IRARL = 0.83 of the FIR AIB-EDC and FIR AIB-EDCC charts are smaller than IRARL = 0.92 and IRARL = 0.90 of the FIR DC and DCC charts. In addition, for comparison of Tables 3 and 6, it is noted that the FIR-based charts in Table 6 surpass the charts without FIR features in Table 3 to detect shifts in a whole range. For example, when $\lambda = 0.5$, the IRARL of the FIR-DC, FIR-DCC, FIR-EDC, FIR-EDCC, FIR AIB-EDC, and FIR-EDCC charts are 0.92, 0.90, 0.95, 0.95, 0.83, and 0.83, respectively (see the last row in Table 6). These values are all smaller than the corresponding IRARL values in the last row of Table 3.

The two-sided charts are presented in Table 7; it can be concluded that two-sided AIB-EDC and AIB-EDCC charts also perform better than the charts without AIB and DC and DCC charts for the detection of a whole range of shifts. For example, at $\lambda = 0.5$, the IRARL are 1.19 and 1.18 for AIB-EDC and AIB-EDCC charts, whereas the IRARL = 1.33 and IRARL = 1.31 of DC and DCC charts, respectively. For the specific shift, the two-sided AIB-EDC and AIB-EDCC

control charts perform better than the two-sided DC, DCC, EDC, and EDCC charts. For example, at $\delta = 0.25, \lambda = 0.75$, and $\rho = 0.75$, the AIB-EDC, AIB-EDCC, DC, and DCC charts produce ARL values of 47.34, 46.48, 144.35, 142.42, 64.81, and 64.68, respectively (see Table 7). Compared with the one-sided charts, it can be noted that all the one-sided charts perform better than the corresponding two-sided charts. For example, when $\lambda = 0.5$, all the ARL/MRL/SDRL values of the one-sided DC, DCC, EDC, EDCC, and AIB-EDC charts for a specific shift δ are smaller than the ones of the corresponding two-sided charts and the IRARL of one-sided charts are also smaller than the IRARL of two-sided charts.

5. Illustrative Example

This section considers an illustrative example to demonstrate the implementation of the proposed charts in real-life scenarios by using the film thickness dataset. The film thickness is one of the prime quality characteristics for coating purposes. The film is a coating material used for protection over reflection to absorption, permeation, transparency, flexibility, transmission, and electrical polarization. Film material is used in many products and technologies such as packaging, sensors, semiconductors, photovoltaics, displays, and biological and medical devices and equipment. The deepness of the coating applied is

known as the film thickness, and generally, it can be classified into two major categories based on the time at which it has been applied: wet film thickness (WFT) and dry film thickness (DFT). The thickness of liquid-based coating like wet paints is known as wet film thickness. Initially, when the coating is applied, it has the wettest thickness but gradually decreases with the evaporation of solvents from the film coating. In order to acquire the particular level of dry film thickness, it is essential to determine the quantity of the material applied while providing the best possible protection against damage and corrosion. After the coating has dried, its level of thickness is measured on top of the layer, which refers to dry film thickness (DFT). The number of layers could be more than one.

DFT is measured only when the coating dries completely. The process which is adopted for the application of coating determines the thickness of the coating. By following the approved coating parameters, a proper level of thickness can be achieved. A manufacturing process produces a polymer film that is in the shape of a rectangle. As a quality control measure for each film produced, the thickness (microns) is measured in four specified locations: bottom left, bottom right, top left, and top right. According to our data of a plastic film thickness after being cut, we can measure the thickness by using the Gauge model 4000/F. Gauge model 4000/F can measure the thickness in the range of “0.001 mm” to “1 mm.” In addition, including the depth of the jaw “35 mm,” and this model is special for measuring like polyethylene bags and thickness of the plastic film and many more things. Here, we consider two variables for the brevity of discussion: X (study variable) top thickness and Y (auxiliary variable) as the bottom thickness measurements from this process. One hundred sixty samples for these variables are used, and the correlation between these variables is 0.75. The data are taken from <https://openmv.net/info/film-thickness>. We standardized both variables before being used for control charting. For illustration purposes, we used four charts, i.e., AIB-EDC, AIB-EDCC, DC, and DCC charts. For a fair comparison, the control limits are adjusted so that all the control charts have the same $ARL_0 = 300$. Specifically, we used $(k_1 = 0.22, k_2 = 0.41, h_1 = 8.5727, \text{ and } h_2 = 4.6000)$ for the one-sided DC $(k_1 = 0.22, k_2 = 0.41, h_1 = 7.7566, \text{ and } h_2 = 4.1621)$ for the DCC $(k_1 = 0.22, k_2 = 0.41, h_1 = 48.4500, \text{ and } h_2 = 26.0000)$ for AIB-EDC and $(k_1 = 0.22, k_2 = 0.41, h_1 = 48.2000, \text{ and } h_2 = 25.8600)$ AIBEDCC charts, considering $\lambda = 0.05$ and $\rho = 0.75$. These control charts are designed to efficiently detect the mean shift δ in the range [0.25, 1]. To check the detection ability of the four charts, shift $\delta = 0.5$ is introduced in the last 30 samples, and the resulting control charts are presented in Figure 1. We can observe from Figure 1 that the proposed AIB-EDC and AIB-EDCC charts detect 18 out-of-control signals, whereas DC and DCC charts detect only 3 and 11 signals, respectively. This superiority of the proposed charts over the existing charts is in accordance with the findings of the simulation study.

6. Conclusions and Recommendations

The Crosier-CUSUM (CC) is the advanced version of the CUSUM chart used to monitor the process when the shift is

not known in advance. Similarly, the mixed EWMA-double CUSUM (EDC) is very efficient for the monitoring of process mean. This paper integrated double CC (DCC) and EWMA chart structures and proposed a new mixed EWMA-DCC (EDCC) charting scheme for monitoring the process mean. In addition, the performance of AIB EDC and mixed EWMA-DCC (EDCC) charts is also investigated for efficient process monitoring. Monte Carlo simulations are used to compute the run-length characteristics of the proposed charts. The ARL, SDRL, MRL, EQL, and IRARL are used as performance measures of the proposed control charts. The proposed one-sided or two-sided EDC and EDCC charts with AIB outperform the existing control charts for different shifts. To guard against the initial/startup problems in the process, FIR features are attached to different control charts, and the results show that the FIR AIB-EDC and AIB-EDCC charts are better than other FIR charts in the detection of a whole range of shifts. The current study can be extended to nonnormal, nonparametric, neutrosophic, and multivariate scenarios.

Data Availability

The data for the study can be provided from the corresponding author on reasonable request.

Conflicts of Interest

The authors declare that they have no conflicts of interest.

References

- [1] W. A. Shewhart and D. Van Nostrand, *Economic Control of Quality Manufactured Product*, reprinted by the American Society for Quality Control in 1980, Milwaukee, WI, 1931.
- [2] E. S. Page, “Continuous inspection schemes,” *Biometrika*, vol. 41, no. 1-2, pp. 100–115, 1954.
- [3] S. W. Roberts, “Control chart tests based on geometric moving averages,” *Technometrics*, vol. 1, no. 3, pp. 239–250, 1959.
- [4] N. Abbas, M. Riaz, and R. J. M. M. Does, “An EWMA-type control chart for monitoring the process mean using auxiliary information,” *Communications in Statistics - Theory and Methods*, vol. 43, no. 16, pp. 3485–3498, 2014.
- [5] A. Haq, “A new adaptive EWMA control chart using auxiliary information for monitoring the process mean,” *Communications in Statistics - Theory and Methods*, vol. 47, no. 19, pp. 4840–4858, 2018.
- [6] S. Abbasi and A. Haq, “Optimal CUSUM and adaptive CUSUM charts with auxiliary information for process mean,” *Journal of Statistical Computation and Simulation*, vol. 89, no. 2, pp. 337–361, 2019.
- [7] A. Haq and M. B. C. Khoo, “Memory-type multivariate control charts with auxiliary information for process mean,” *Quality and Reliability Engineering International*, vol. 35, no. 1, pp. 192–203, 2019.
- [8] A. Riaz, M. Noor-ul-Amin, M. A. Shehzad, and M. Ismail, “Auxiliary information based mixed EWMA-CUSUM mean control chart with measurement error,” *Iranian Journal of Science and Technology Transaction A-Science*, vol. 43, no. 6, pp. 2937–2949, 2019.

- [9] M. Aslam, M. Azam, N. Khan, and C.-H. Jun, "A mixed control chart to monitor the process," *International Journal of Production Research*, vol. 53, no. 15, pp. 4684–4693, 2015.
- [10] M. Aslam, "A mixed EWMA-CUSUM control chart for w-distributed quality characteristics," *Quality and Reliability Engineering International*, vol. 32, no. 8, pp. 2987–2994, 2016.
- [11] M. Aslam, N. Khan, M. S. Aldosari, and C.-H. Jun, "Mixed control charts using EWMA statistics," *IEEE Access*, vol. 4, pp. 8286–8293, 2016.
- [12] A. Haq and L. Bibi, "The dual CUSUM charts with auxiliary information for process mean," *Communications in Statistics - Simulation and Computation*, vol. 51, no. 1, pp. 164–189, 2022.
- [13] S. M. Anwar, M. Aslam, M. Riaz, and B. Zaman, "On mixed memory control charts based on auxiliary information for efficient process monitoring," *Quality and Reliability Engineering International*, vol. 36, no. 6, pp. 1949–1968, 2020.
- [14] S. M. Anwar, M. Aslam, S. Ahmad, and M. Riaz, "A modified-mxEWMA location chart for the improved process monitoring using auxiliary information and its application in wood industry," *Quality Technology & Quantitative Management*, vol. 17, no. 5, pp. 561–579, 2020.
- [15] M. Aslam, N. Khan, L. Ahmad, C.-H. Jun, and J. Hussain, "A mixed control chart using process capability index," *Sequential Analysis*, vol. 36, no. 2, pp. 278–289, 2017.
- [16] S. Lee, "Location and scale-based CUSUM test with application to autoregressive models," *Journal of Statistical Computation and Simulation*, vol. 90, no. 13, pp. 2309–2328, 2020.
- [17] M. Abid, S. Mei, H. Z. Nazir, M. Riaz, and S. Hussain, "A mixed HWMA-CUSUM mean chart with an application to manufacturing process," *Quality and Reliability Engineering International*, vol. 37, no. 2, pp. 618–631, 2021.
- [18] M. Khan, M. Aslam, S. M. Anwar, and B. Zaman, *A Robust Hybrid Exponentially Weighted Moving Average Chart for Monitoring Time between Events*, Quality and Reliability Engineering International, New Jersey, USA, 2021.
- [19] A. Haq, M. B. C. Khoo, M. Ha Lee, and S. A. Abbasi, "Enhanced adaptive multivariate EWMA and CUSUM charts for process mean," *Journal of Statistical Computation and Simulation*, vol. 91, no. 12, pp. 2361–2382, 2021.
- [20] S. Hussain, M. Sun, T. Mahmood, M. Riaz, and M. Abid, "IQR CUSUM charts: an efficient approach for monitoring variations in aquatic toxicity," *Journal of Chemometrics*, vol. 35, no. 5, Article ID e3336, 2021.
- [21] S. M. Anwar, M. Aslam, B. Zaman, and M. Riaz, "Mixed memory control chart based on auxiliary information for simultaneously monitoring of process parameters: an application in glass field," *Computers & Industrial Engineering*, vol. 156, Article ID 107284, 2021.
- [22] Y. Zhao, F. Tsung, and Z. Wang, "Dual CUSUM control schemes for detecting a range of mean shifts," *IIE Transactions*, vol. 37, no. 11, pp. 1047–1057, 2005.
- [23] M. Hany and M. A. Mahmoud, "An evaluation of the Crosier's CUSUM control chart with estimated parameters," *Quality and Reliability Engineering International*, vol. 32, no. 5, pp. 1825–1835, 2016.
- [24] A. Haq and W. Munir, "Improved CUSUM charts for monitoring process mean," *Journal of Statistical Computation and Simulation*, vol. 88, no. 9, pp. 1684–1701, 2018.
- [25] N. Abbas, I. A. Raji, M. Riaz, and K. Al-Ghamdi, "On designing mixed EWMA dual-CUSUM chart with applications in petro-chemical industry," *IEEE Access*, vol. 6, pp. 78931–78946, 2018.
- [26] Z. Song, A. Mukherjee, and J. Zhang, "An efficient approach of designing distribution-free exponentially weighted moving average schemes with dynamic fast initial response for joint monitoring of location and scale," *Journal of Statistical Computation and Simulation*, vol. 90, no. 13, pp. 2329–2353, 2020.
- [27] S. Saha, A. Mukherjee, and M. B. C. K. Khoo, *Two CUSUM Schemes for Simultaneous Monitoring of Unknown Parameters of a Shifted Exponential Process and its Application in Monitoring of Call Durations in Telemarketing*, Quality Technology & Quantitative Management, vol. 19, no. 1, pp. 113–137, 2022.
- [28] A. Haq and E. A. Syed, "New CUSUM and dual CUSUM mean charts," *Quality and Reliability Engineering International*, vol. 37, no. 4, pp. 1355–1372, 2021.
- [29] S. Haridy, M. Shamsuzzaman, I. Alsayouf, and A. Mukherjee, "An improved design of exponentially weighted moving average scheme for monitoring attributes," *International Journal of Production Research*, vol. 58, no. 3, pp. 931–946, 2020.
- [30] I. A. Raji, M. Riaz, and N. Abbas, "Robust dual-CUSUM control charts for contaminated processes," *Communications in Statistics - Simulation and Computation*, vol. 48, no. 7, pp. 2177–2190, 2019.
- [31] A. Haq and L. Bibi, "A new dual CUSUM mean chart," *Quality and Reliability Engineering International*, vol. 35, no. 4, pp. 1245–1262, 2019.
- [32] A. Javaid, M. Noor-ul-Amin, and M. Hanif, "A new Max-HEWMA control chart using auxiliary information," *Communications in Statistics - Simulation and Computation*, vol. 49, no. 5, pp. 1285–1305, 2020.
- [33] M. Aslam and S. M. Anwar, "An improved Bayesian Modified-EWMA location chart and its applications in mechanical and sport industry," *PLoS One*, vol. 15, no. 2, Article ID e0229422, 2020.
- [34] Z. Rasheed, H. Zhang, S. M. Anwar, and B. Zaman, "Homogeneously mixed memory charts with application in the substrate production process," *Mathematical Problems in Engineering*, vol. 2021, Article ID 2582210, 15 pages, 2021.
- [35] J. M. Lucas and R. B. Crosier, "Fast initial response for CUSUM quality-control schemes: give your CUSUM a head start," *Technometrics*, vol. 24, no. 3, pp. 199–205, 1982.
- [36] R. B. Crosier, "A new two-sided cumulative sum quality control scheme," *Technometrics*, vol. 28, no. 3, pp. 187–194, 1986.
- [37] M. Riaz, "Monitoring process mean level using auxiliary information," *Statistica Neerlandica*, vol. 62, no. 4, pp. 458–481, 2008.
- [38] Z. Wu, J. Jiao, M. Yang, Y. Liu, and Z. Wang, "An enhanced adaptive CUSUM control chart," *IIE Transactions*, vol. 41, no. 7, pp. 642–653, 2009.
- [39] K. Tanaka, F. Sato, H. Oodaira, Y. Teranishi, F. Sato, and S. Ujihashi, "Construction of the finite-element models of golf balls and simulations of their collisions," *Proceedings of the Institution of Mechanical Engineers - Part L: Journal of Materials: Design and Applications*, vol. 220, no. 1, pp. 13–22, 2006.